Modèle géométrique et intégration biomécanique : quelques réflexions

Gérard Subsol
CNRS, LIRMM, Montpellier
gerard.subsol@lirmm.fr

Guillaume Captier
Laboratoire d'Anatomie, Faculté de Médecine de Montpellier

Karim Fathi
Master 1 EEA, Université de Montpellier 2

Avec l'aide *de Benjamin Gilles*, CNRS, LIRMM, Montpellier qui précisera, développera et prolongera….

1. Comment modéliser la géométrie du muscle ?
2. Comment obtenir les paramètres géométriques ?
3. Une loi “classique” du muscle ?
4. Des modèles alternatifs ?
5. Une modélisation simple qui soulève des questions…
6. Quelques-unes de ces questions

ELSEVIER

PII: S0021-9290(97)00058-4

J. Biomechanics, Vol. 30, No. 9, pp. 943–950, 1997

Printed in Great Britain
0021-9290/97 $17.00 + .00

THE JAW OPEN–CLOSE MOVEMENTS PREDICTED BY BIOMECHANICAL MODELLING

J. H. Koolstra,* and T. M. G. J. van Eijden

Department of Functional Anatomy, Academic Centre for Dentistry Amsterdam (ACTA), Meibergdreef 15, 1105 AZ Amsterdam, The Netherlands

1D model (l_i)(1)

- Muscle = 1 **straight** line of action

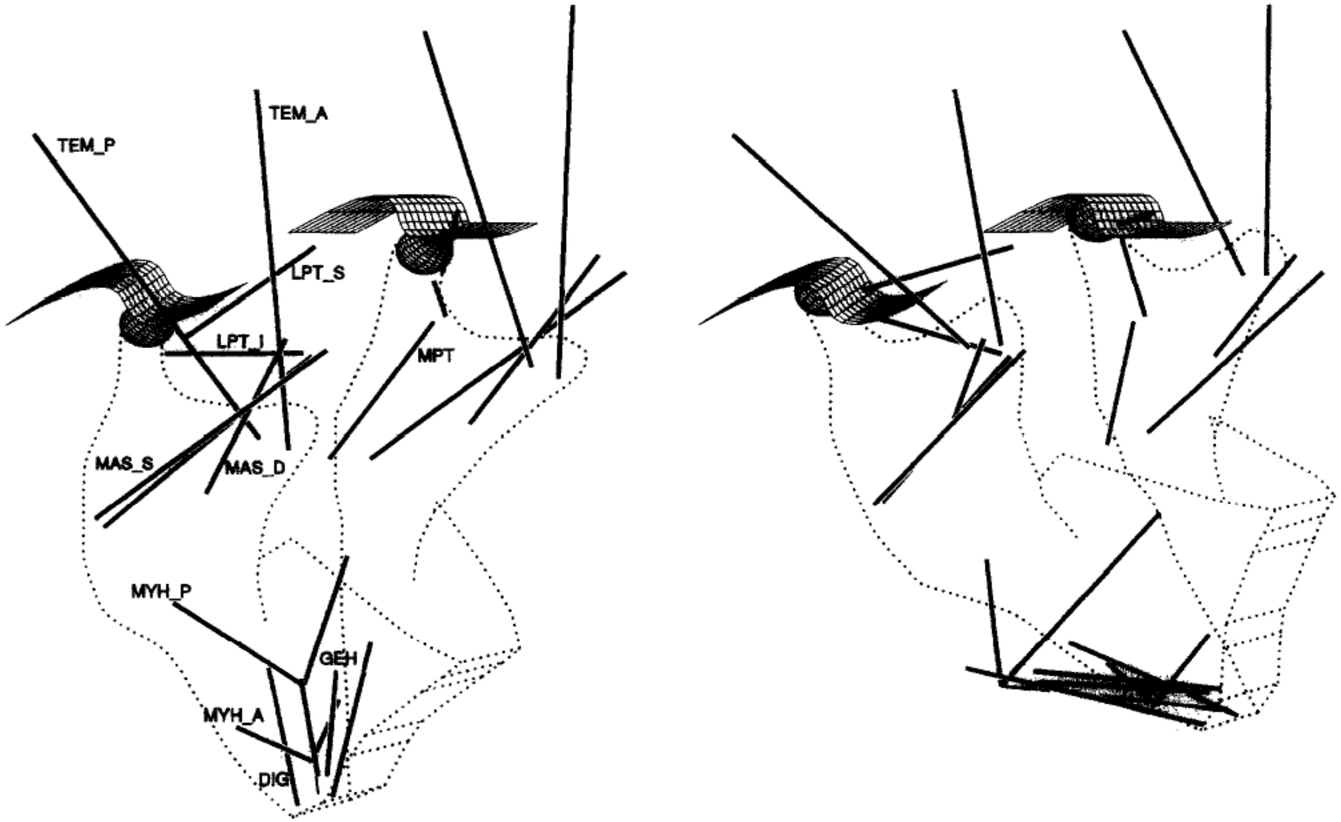

Fig. 1. Overview of the model. The dark lines represent muscle lines of action in the open position (left panel) and in the closed position (right panel). MAS_S = superficial masseter, MAS_D = deep masseter, MPT = medial pterygoid, TEM_A = anterior temporalis, TEM_P = posterior temporalis, LPT_S = superior lateral pterygoid, LPT_I = inferior lateral pterygoid, DIG = digastric, GEH = geniohyoid, MYH_A = anterior mylohyoid, MYH_P = posterior mylohyoid.

1D model (l_i) (2)

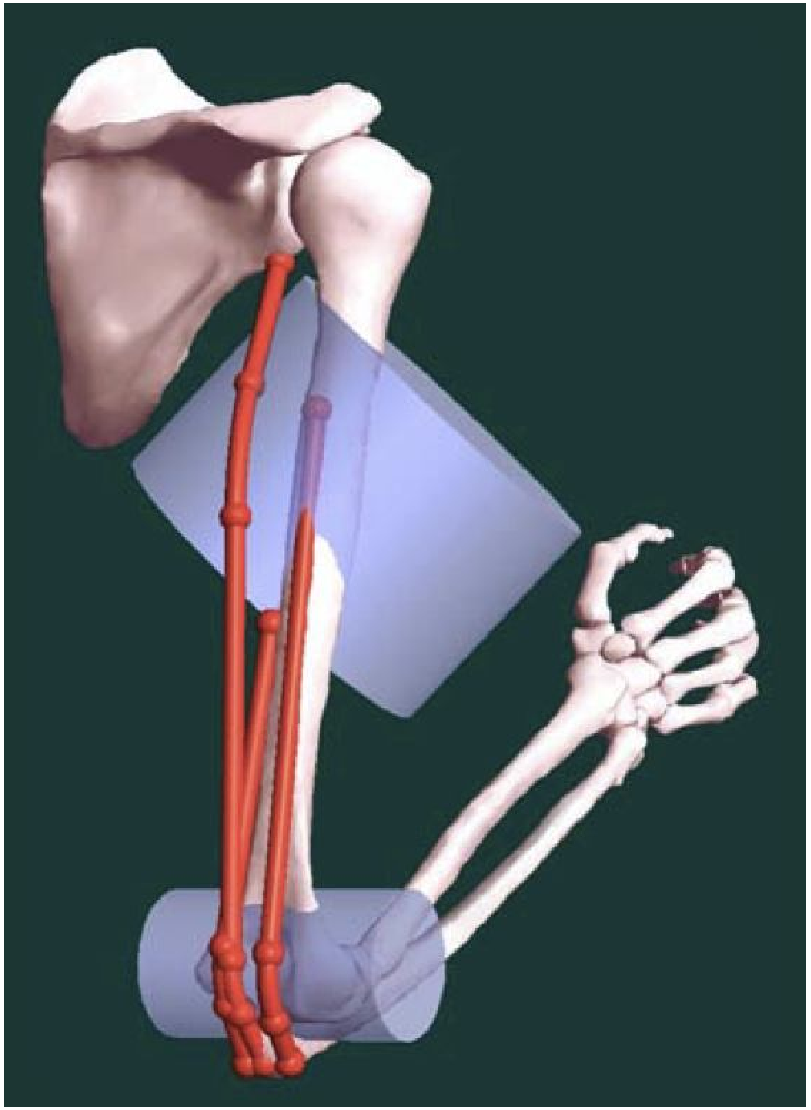

Computer Methods in Biomechanics and Biomedical Engineering, Vol. 3, pp. 1–30
Reprints available directly from the publisher
Photocopying permitted by license only

The Obstacle-Set Method for Representing Muscle Paths in Musculoskeletal Models

BRIAN A. GARNER and MARCUS G. PANDY*

- 1D muscle
- Deals dynamically with obstacles by **wrapping** along the bone and joints which are represented by cylinders or spheres

2D model (f_i,l_i)

Computer Methods in Biomechanics and Biomedical Engineering, Vol. 9, No. 6, December 2006, 387–398

Taylor & Francis
Taylor & Francis Group

Computational model of the movement of the human muscles of mastication during opening and closing of the jaw

LAETITIA M. M. LEON†, BERNARD LIEBGOTT‡*, ANNE M. AGUR‡ and KENNETH H. NORWICH†

- Modeling a bundle (several hundred fibers)
- Based on dissection
- Recording of 3D coordinates by a MicroScribe digitizer (origin and insertion + 6-12 intervening points)
- Detection of collision and wrapping around bony parts

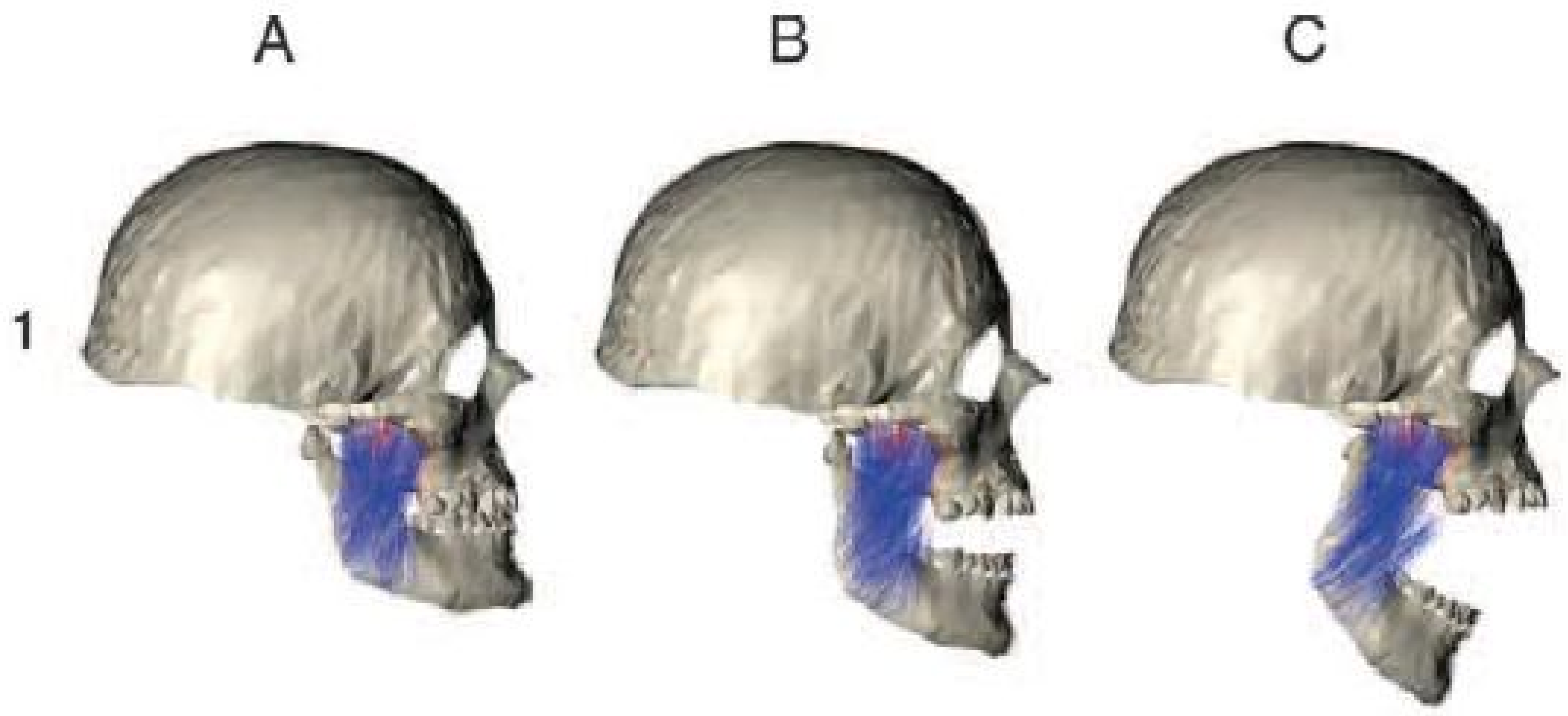

3D model (*x,y,z*) (1)

Computer Graphics, 26, 2, July 1992

**Pump It Up:
Computer Animation of a Biomechanically Based
Model of Muscle Using the Finite Element Method**

- Global volume model
- For computer-graphics application, requirement of 3D visualization
- FEM resolution based on a Zajac muscle model
- **Not based** on a specific definition of the muscle fibers

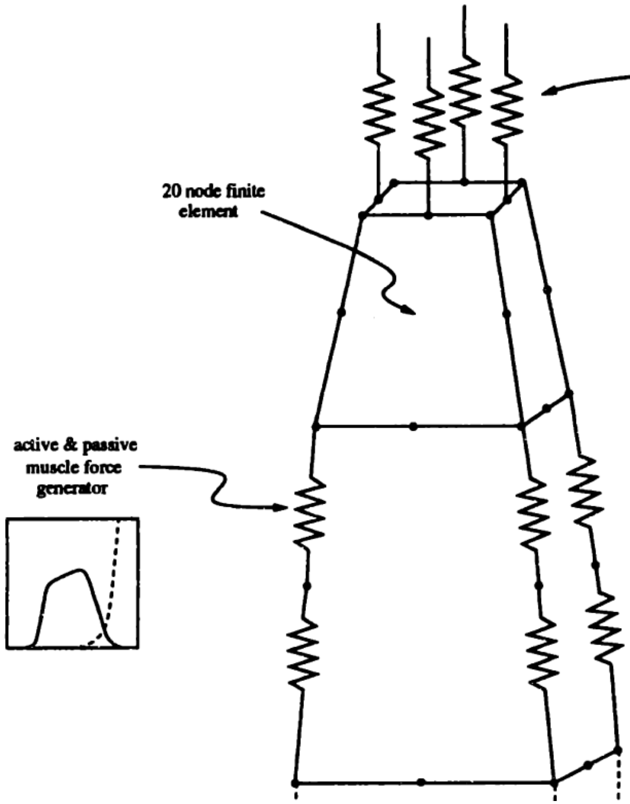

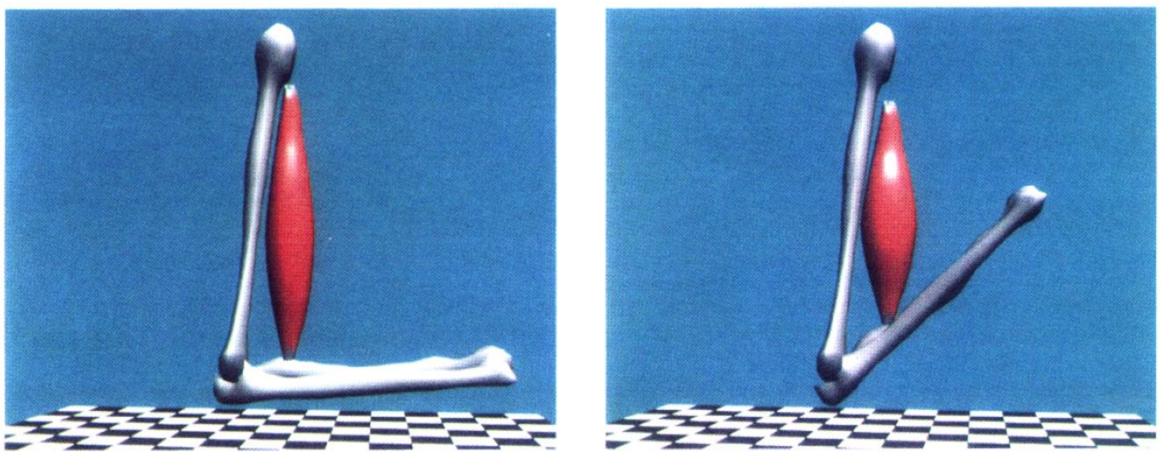

Figure 17: Biceps shortens upon activation, forearm motion is specified inverse kinematically.

Annals of Biomedical Engineering, Vol. 33, No. 5, May 2005 (© 2005) pp. 661–673
DOI: 10.1007/s10439-005-1433-7

3D model (*x,y,z*) (2)

- The fiber architecture is specifically modeled

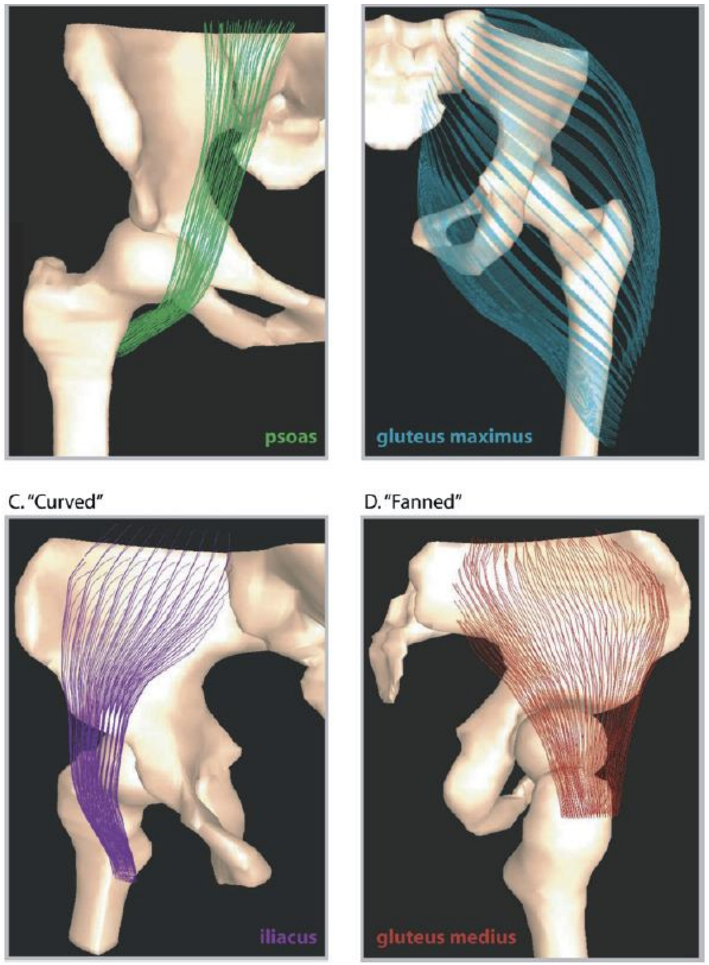

FIGURE 5. Examples of fiber geometries mapped to the psoas (A), gluteus maximus (B), iliacus (C), and gluteus medius (D) muscles.

Three-Dimensional Representation of Complex Muscle Architectures and Geometries

SILVIA S. BLEMKER and SCOTT L. DELP

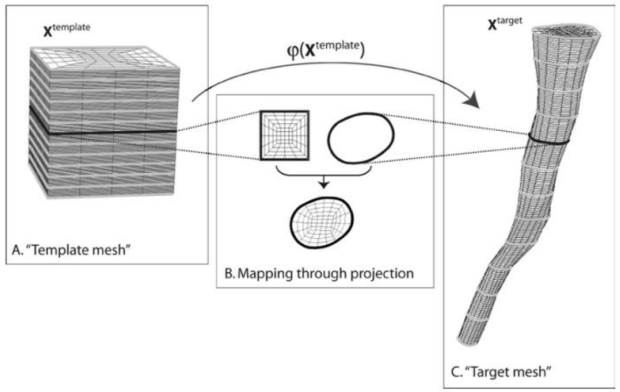

FIGURE 3. Creation of volumetric meshes of each muscle from segmented surface models. Hexahedral meshes were created by mapping a "template" hexahedral mesh (A) through a series of projections (B) to the "target" mesh (C). Each slice of the mesh corresponds to an outline of an anatomical structure created during segmentation (see Fig. 2).

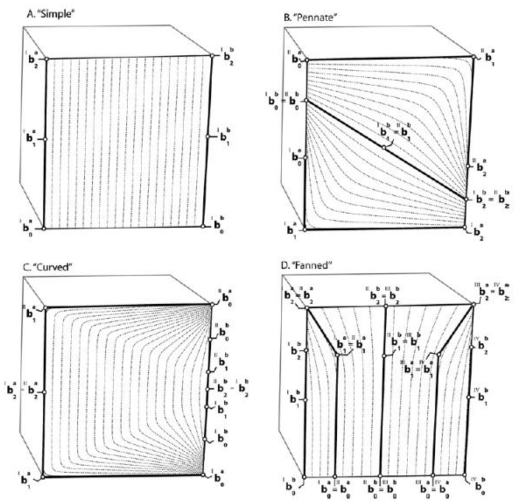

FIGURE 4. Fiber geometry templates used for parallel muscles (A), pennate muscles (B), curved muscles (C), and fanned muscles (D). The templates consist of interpolated rational Bezier spline curves. In the simplest case (A), only one set of spline curves are the basis for the interpolation. In the most complex case (D), four sets of spline curves are the basis for the interpolation.

3D architectural model

- The fiber architecture is specifically modeled

ELSEVIER

Journal of Biomechanics 40 (2007) 3363–3372

JOURNAL OF BIOMECHANICS

www.elsevier.com/locate/jbiomech
www.JBiomech.com

Three-dimensional finite element modelling of muscle forces during mastication

Oliver Röhrle[a,*], Andrew J. Pullan[a,b]

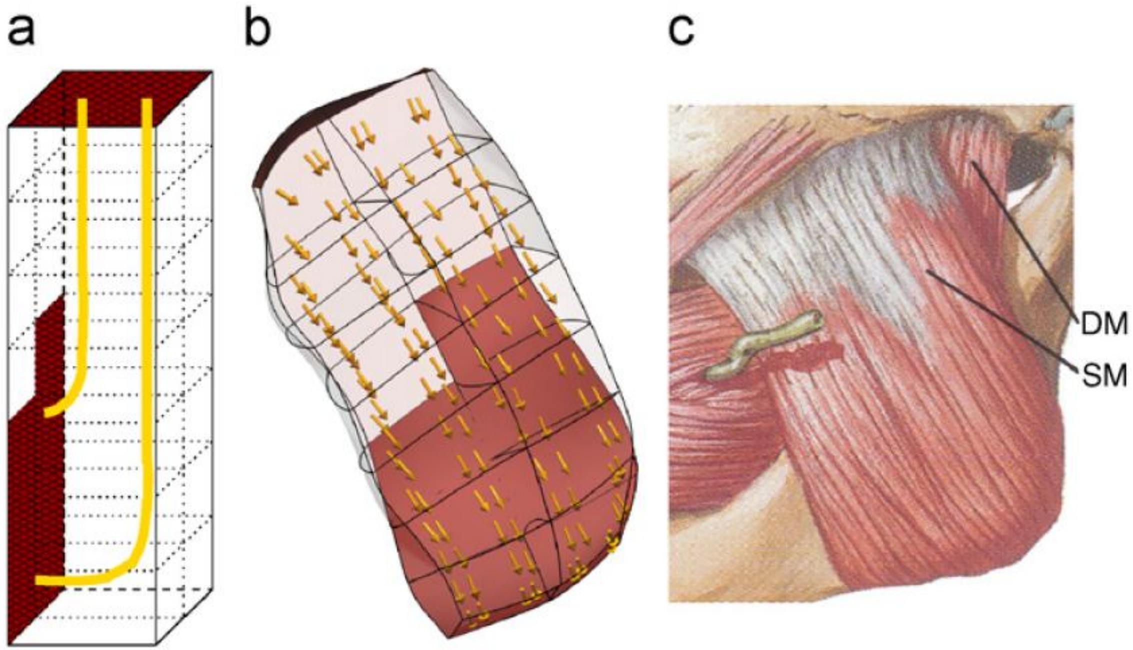

Fig. 3. Directions of the fibre field in (a) the template, (b) within the final geometry, and (c) schematic drawing of the deep (DM) and superficial masseter (SM) (from Netter, 2003). In (a) and (b), the attachment areas of the muscle to the mandible (on the left) and maxilla (on the top) are shown in red.

3D geometric modeling from dissection

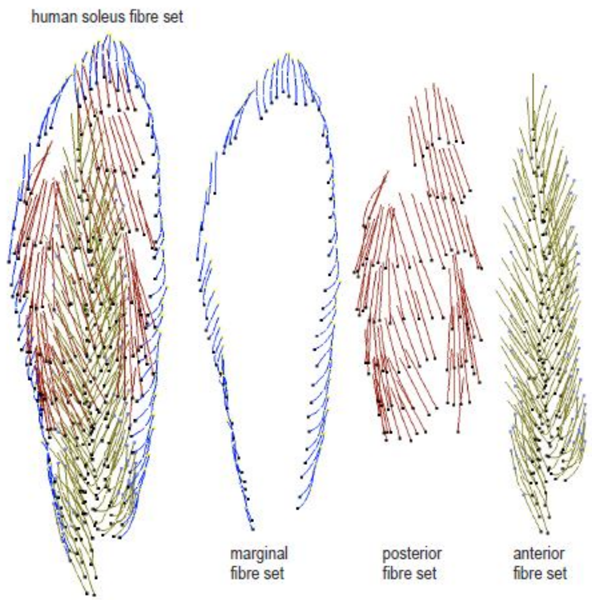

Figure 4: Digitized fibre sets for the three regions of human soleus

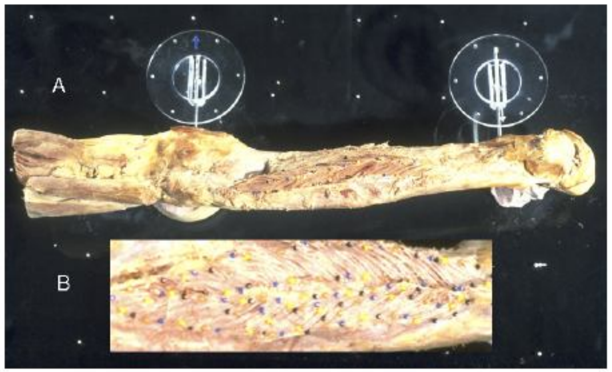

Figure 5: Serial dissection of human soleus muscle with marked fibre points

Clinical Anatomy 16:285–293 (2003)

ORIGINAL COMMUNICATION

Documentation and Three-Dimensional Modelling of Human Soleus Muscle Architecture

ANNE M. AGUR,[1]* VICTOR NG-THOW-HING,[2] KEVIN A. BALL,[3] EUGENE FIUME,[2] AND NANCY HUNT McKEE[4]

3D geometric modeling from CT

Osirix Web site

3D geometric modeling from MR

JOURNAL OF MAGNETIC RESONANCE IMAGING 25:441–451 (2007)

Invited Review

Image-Based Musculoskeletal Modeling: Applications, Advances, and Future Opportunities

Silvia S. Blemker, PhD,[1,5*] Deanna S. Asakawa, PhD,[2] Garry E. Gold, MD,[4] and Scott L. Delp, PhD[2,3]

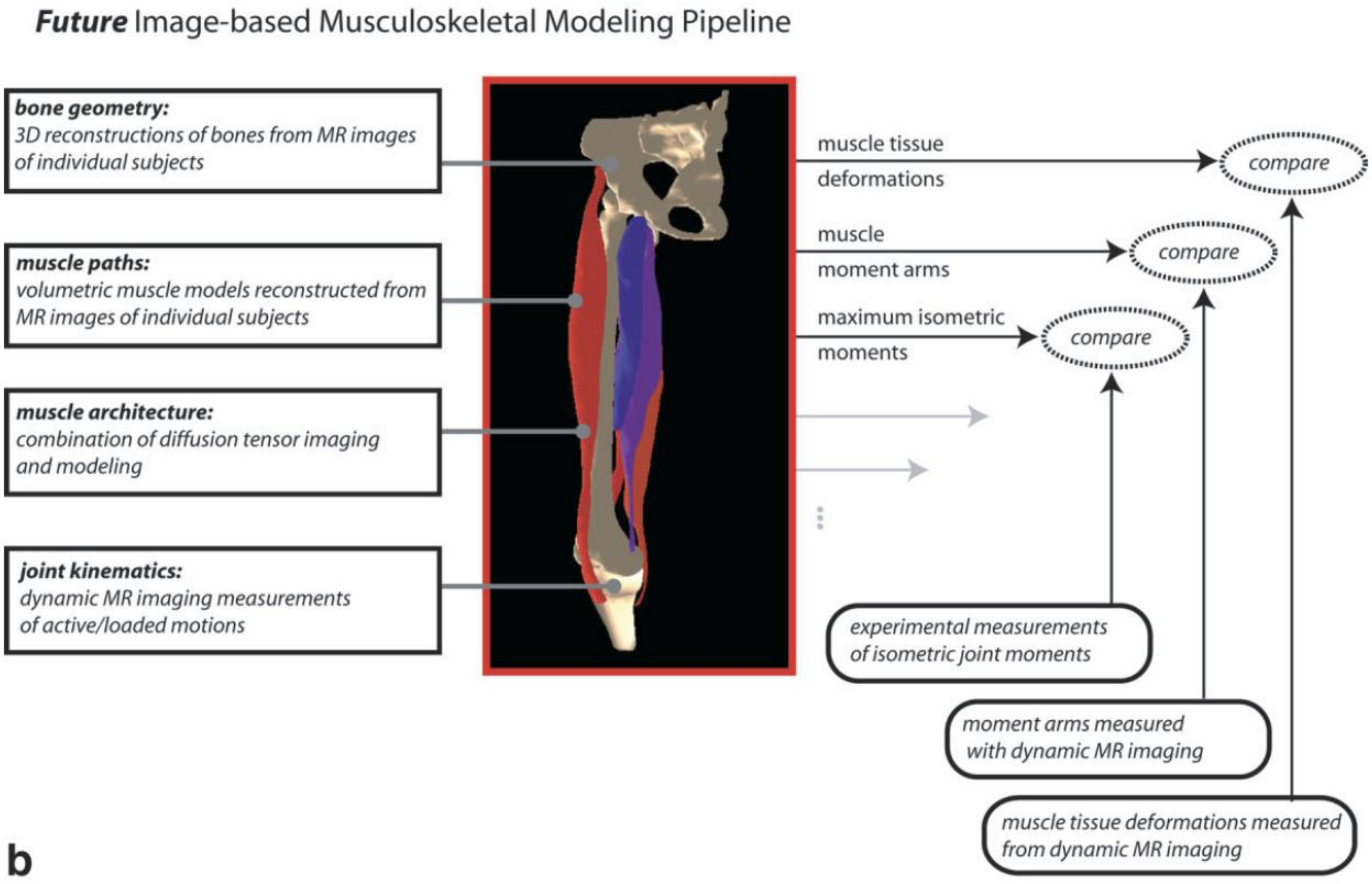

3D geometric modeling from ultrasound

See:

10h30-11h00 Exploration des fibres musculaires par échographie et IRM.
Ahmed Larbi, département de radiologie ostéoarticulaire, CHRU Montpellier

Determination of fascicle length and pennation in a contracting human muscle in vivo

Tetsuo Fukunaga, Yoshiho Ichinose, Masamitsu Ito, Yasuo Kawakami and Senshi Fukashiro

J Appl Physiol 82:354-358, 1997.

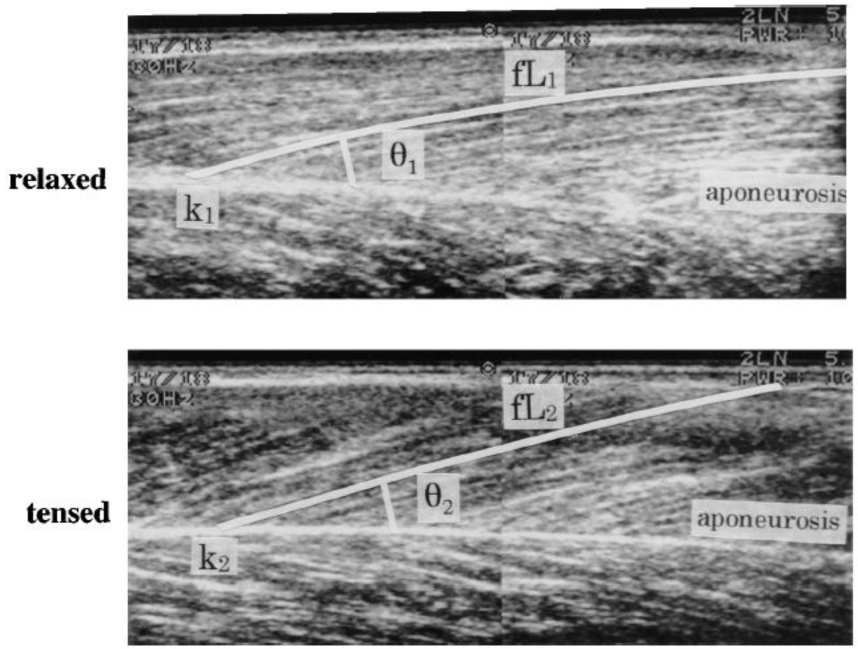

Fig. 1. Ultrasonic longitudinal image of vastus lateralis muscle. Ultrasonic transducer was placed on skin over the muscle at 50% distance from greater trochanter to lateral epicondyle of femur. Fascicle length (fL) was determined as length of a line drawn along ultrasonic echo parallel to fascicle. Fascicle angle (θ) was determined as angle between echoes obtained from fascicles and deep aponeurosis in ultrasonic image. *k*, Distal end of a fascicle.

3D geometric modeling from μ-CT

Journal of Biomechanics 44 (2011) 189–192

Contents lists available at ScienceDirect

Journal of Biomechanics

journal homepage: www.elsevier.com/locate/jbiomech
www.JBiomech.com

Short communication

Micro-computed tomography with iodine staining resolves the arrangement of muscle fibres

Nathan S. Jeffery*, Robert S. Stephenson, James A. Gallagher, Jonathan C. Jarvis, Philip G. Cox

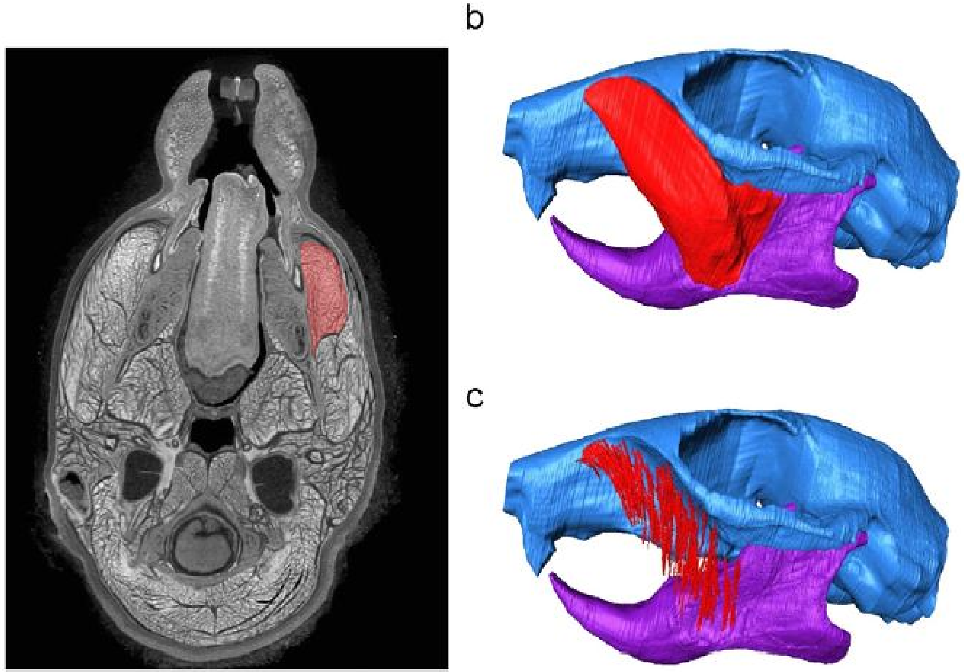

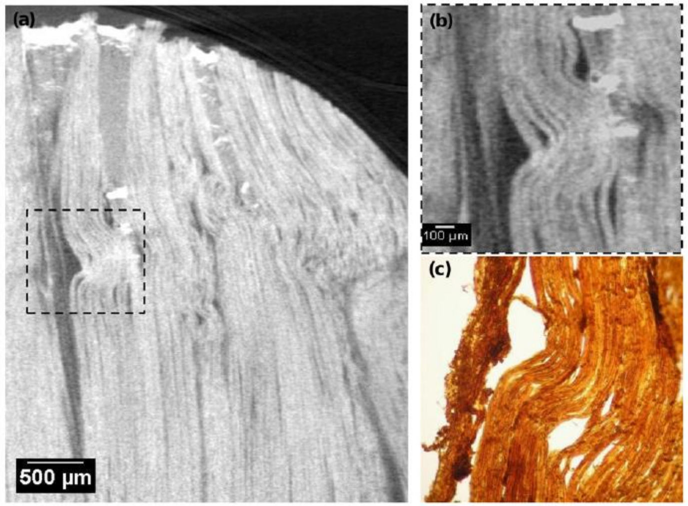

Fig. 4. Longitudinal sections of foetal pig EDL muscle with iodine enhanced micoCT (a, b) and with standard histological sectioning (c). The histological section is stained only with the impregnating iodine, which is clearly taken up by the muscle fibres. Resolution on individual fibres is possible, and registration of fibre orientation is feasible with the microCT.

The Hill-Zajac mechanical model (1)

Critical Reviews in Biomedical Engineering Volume 17, Issue 4 (1989) 359

MUSCLE AND TENDON: PROPERTIES, MODELS, SCALING, AND APPLICATION TO BIOMECHANICS AND MOTOR CONTROL

Author: Felix E. Zajac

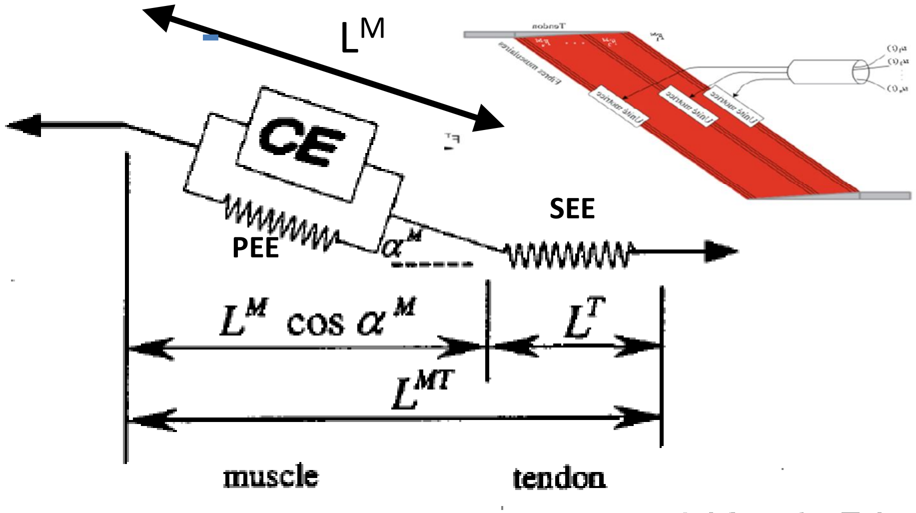

CE: Contractile Element (= active muscle force)

Related to the activation $a(t)$, the muscle fiber length $L^M(t)$ and to its contraction speed $v^M(t)$=d $L^M(t)$/dt :

$$F^{CE}(a, L^M, v^M) = a \cdot F^{CE}_0 \cdot f_l^{CE}(L^M / L^{CE}_0) \cdot f_v^{CE}(L^M / L^{CE}_0)$$

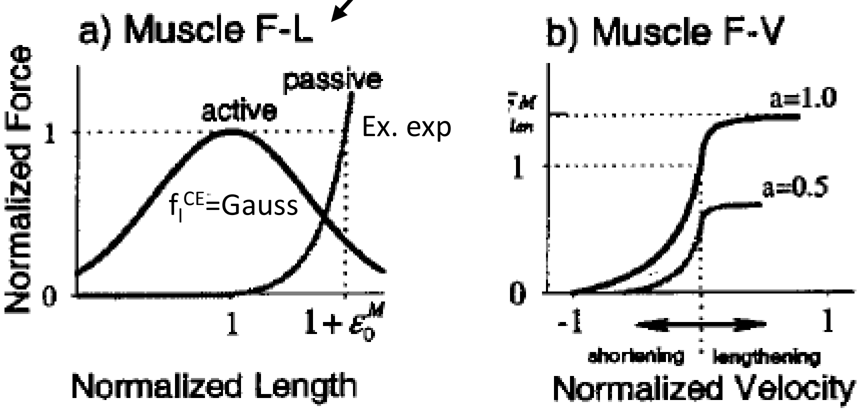

- **Muscle** : $F^M(a, L^M, v^M) = F^{CE}(a, L^M, v^M) + F^{PEE}(L^M)$
- **Tendon** : $F^{SEE}(L^T)$

PEE= Passive Elastic Element (= muscle resistance)

Related to the muscle fiber length $L^M(t)$

$$F^{PEE}(L^M) = F^{CE}_0 \cdot f^{PEE}(L^M / L^{CE}_0)$$

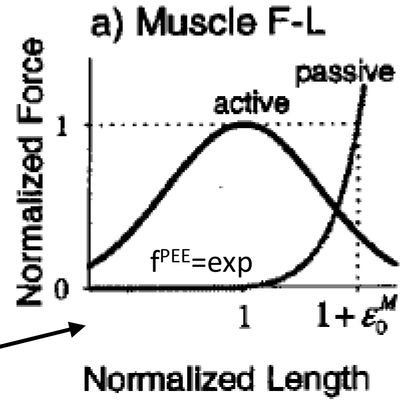

SEE= Serial Elastic Element (= tendon elasticity)

Related to the tendon length $L^M(t)$

$$F^{SEE}(L^T) = F^{CE}_0 \cdot f^T(L^T / L^T_0 - 1) \text{ pour } L^T > L^T_0$$

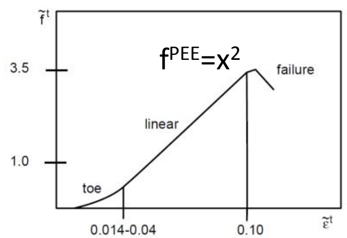

The Hill-Zajac mechanical model (2)

Critical Reviews in Biomedical Engineering Volume 17, Issue 4 (1989) 359

MUSCLE AND TENDON: PROPERTIES, MODELS, SCALING, AND APPLICATION TO BIOMECHANICS AND MOTOR CONTROL

Author: Felix E. Zajac

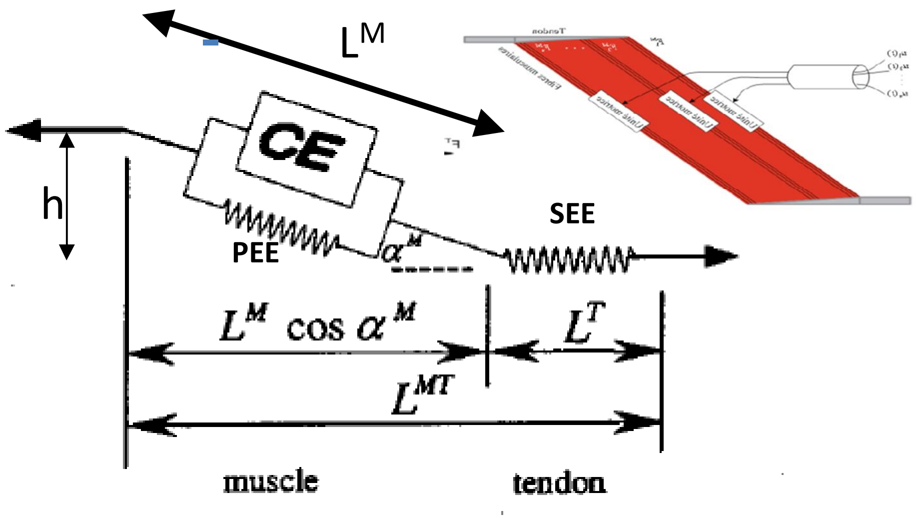

H1: Linear displacement (h=cste)

(1) $\alpha^M(t) = \arcsin(\sin \alpha_0 \,.\, L^{CE}{}_0 / L^M)$

(2) $\mathbf{L^{MT}(t)} = L^T(t) + L^M(t) \,.\, \cos \alpha^M(t)$

H2: Quasi-static (m and a small) :

(3) $\mathbf{F^{MT}}(t) = F^{SEE}(L^T) = F^M(a, L^M, v^M) . \cos \alpha^M(t)$

(1) → $\mathbf{F^{MT}}(t) = F^{SEE}(L^T) = F^M(a, L^M, v^M) \,.\, c(L^M)$

(2) → $\mathbf{F^{MT}}(t) = F^M(a, L^{MT} - L^T, v^{MT} - v^T) \,.\, c(L^{MT} - L^T)$

(3) → $L^T = F^{SEE\,-1}(\mathbf{F^{MT}}(t))$

(2)+(3) → $\mathbf{F^{MT}}(t) = f(a, L^{MT}, v^{MT}, \mathbf{F^{MT}}(t), d\mathbf{F^{MT}}(t)/dt)$

- Static optimization: measurements of body motions → muscle forces
- Dynamic optimization: muscle activation → body motion

Published in *Corpus, Psyche et Societas* **5**, 22-48 1998

Modelling Skeletal Muscle-Tendon Units as Actuators in Motor Behaviour: Morphological Aspects

This mechanical model can be extended, in particular, to take into consideration more precisely the apeunorosis.

Gertjan Ettema

Resolution by FEM

Add an equation to model the effect of the connective tissue and the biofluids surrounding the fibers (= consitutive law):

- Simple: linear (simplistic)

  ….
- More realistic: hyperelastic, incompressible (volume conservation), transversely isotropic

Muscle and Tendon Tissues: Constitutive Modeling and Computational Issues

L. A. Spyrou
e-mail: lspyrou@mie.uth.gr

N. Aravas[1]
Professor, Fellow ASME
e-mail: aravas@mie.uth.gr

Journal of Applied Mechanics JULY 2011, Vol. 78

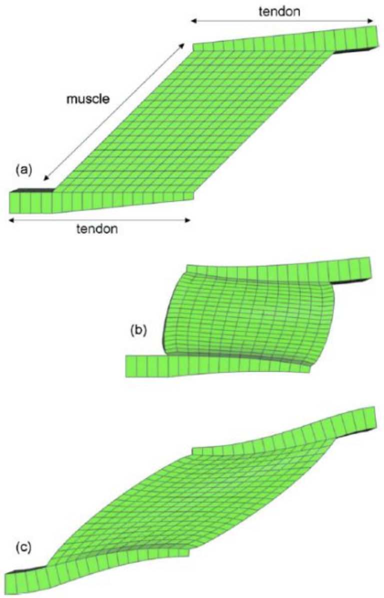

Fig. 14 Pennate muscle. (*a*) Undeformed configuration. (*b*) Concentric contraction. (*c*) Isometric contraction.

ELSEVIER
Journal of Biomechanics 40 (2007) 3363–3372
JOURNAL OF BIOMECHANICS
www.elsevier.com/locate/jbiomech
www.JBiomech.com

Three-dimensional finite element modelling of muscle forces during mastication

Oliver Röhrle[a,*], Andrew J. Pullan[a,b]

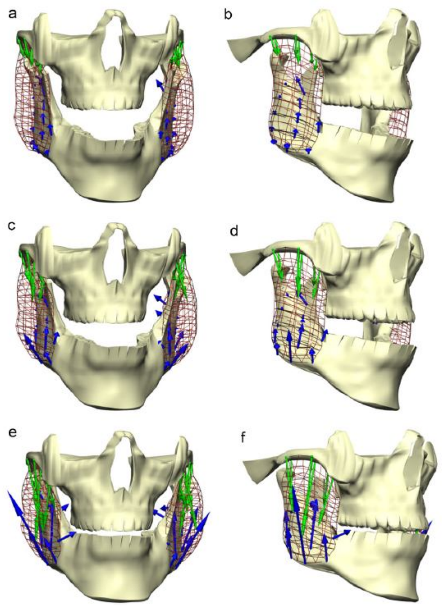

Fig. 5. Front and side views of the mandible, maxilla, and right and left masseter muscles at $t = 0.93$ s, $t = 1.00$ s, and $t = 1.23$ s during the simulation of the chewing cycle depicted in Fig. 2. The green arrows at the maxilla and the blue arrows at the mandible depict the direction of the muscle forces generated at the attachment area. Their lengths are scaled by the magnitude of the calculated muscle force.

Alternative models?

A Survey of Modeling and Simulation of Skeletal Muscle

DONGWOON LEE
Autodesk Research, University of Toronto
MICHAEL GLUECK, AZAM KHAN
Autodesk Research
and
EUGENE FIUME, KEN JACKSON
University of Toronto

- Huxley model (based on physiology)….

- Simplified models (often used for animation real-time applications) as mass-spring systems….

Computer Graphics International - CGI'98, Proceedings (IEEE), p. 156-165, Hannover, Germany, June 22-26, 1998.

Real Time Muscle Deformations Using Mass-Spring Systems

Luciana Porcher Nedel Daniel Thalmann

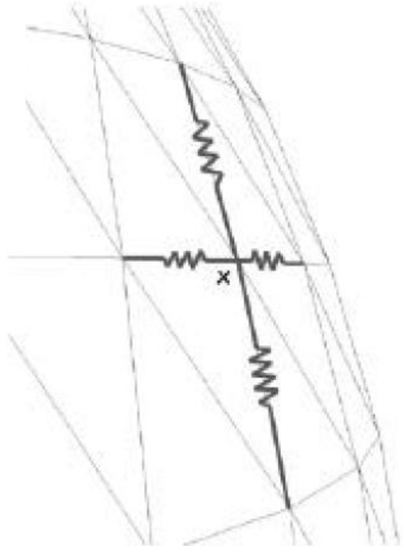

Figure 4. Elastic model of the muscle surface

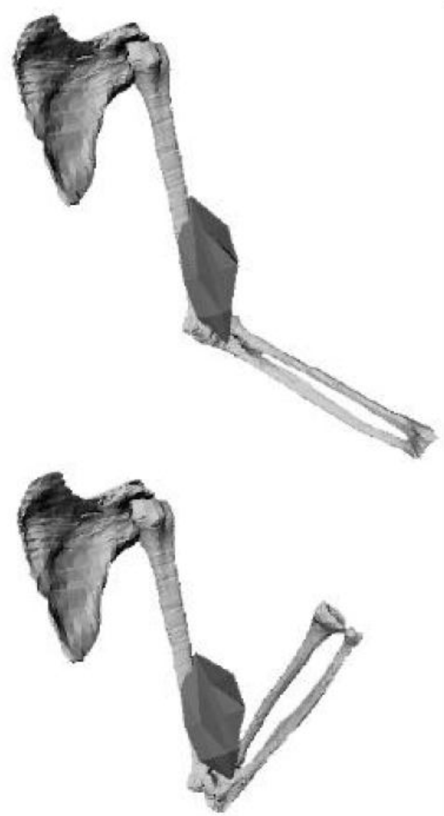

Figure 11. Bones motion with muscle contraction

Modeling a “simple” muscle: the superficial masseter (1)

- Superficial layer:
  - Zygomatic insertion by a strong and thick aponeurosis
  - Maxillar insertion

- Deep layer:
  - Maxillar insertion by an aponeurosis
  - Zygomatic insertion

Surg Radiol Anat 22: 181-190

Original articles

Functional organization of the human masseter muscle

J.-F. Gaudy[1], A. Zouaoui[1], P. Bravetti[2], J.-L. Charrier[1] and A. Guettaf[3]

Surg Radiol Anat (2003) 25: 270–283
DOI 10.1007/s00276-003-0125-y

ORIGINAL ARTICLE

G. Brunel · A. El Haddioui · P. Bravetti
A. Zouaoui · J.-F. Gaudy

General organization of the human intra-masseteric aponeuroses: changes with ageing

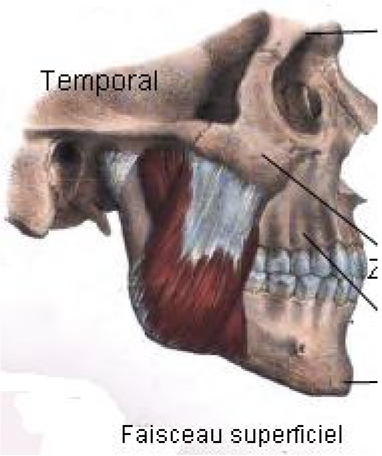

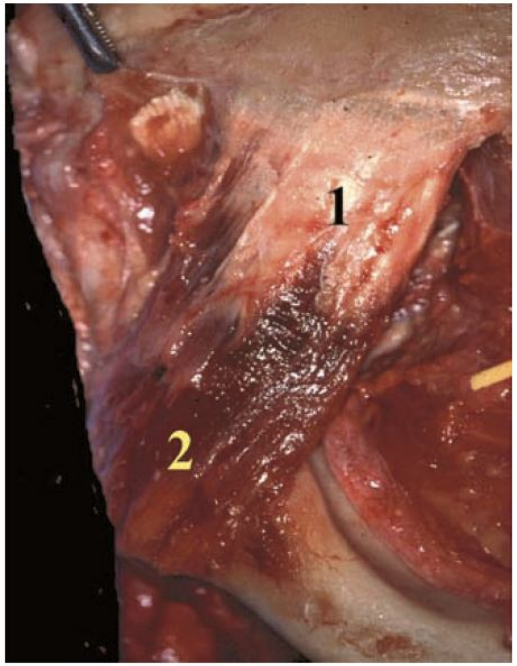

Fig. 2 Superficial masseter muscle, superficial layer (prior lamina). *1*, tendinous sheet; *2*, muscle belly

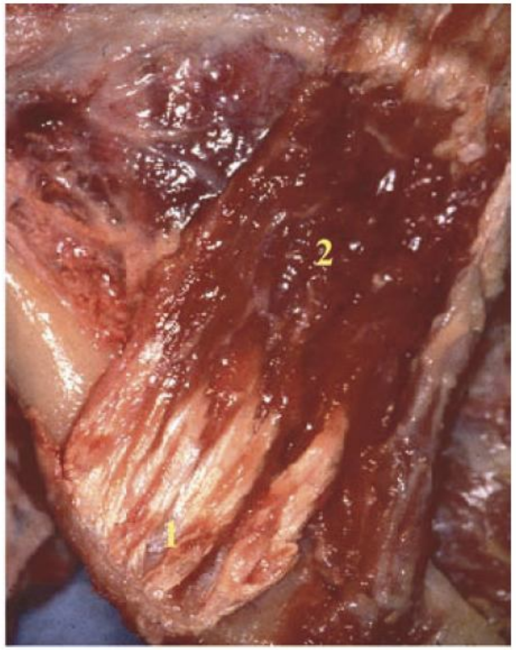

Fig. 3 Superficial masseter, deep layer (altera lamina). *1*, tendinous insertion; *2*, muscle belly

Modeling a “simple” muscle: the superficial masseter (2)

- Superficial layer:
  - Zygomatic insertion by a strong and thick aponeurosis
  - Maxillar insertion

- Deep layer:
  - Maxillar insertion by an aponeurosis
  - Zygomatic insertion

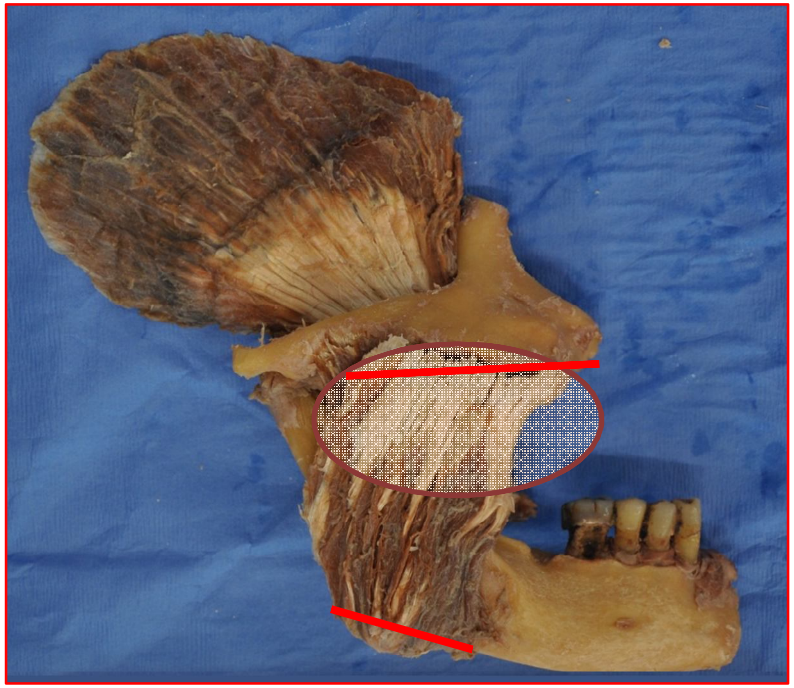

Modeling a "simple" muscle: the superficial masseter (2)

- Superficial layer:
  - Zygomatic insertion by a strong and thick aponeurosis
  - Maxillar insertion

- Deep layer:
  - Maxillar insertion by an aponeurosis
  - Zygomatic insertion

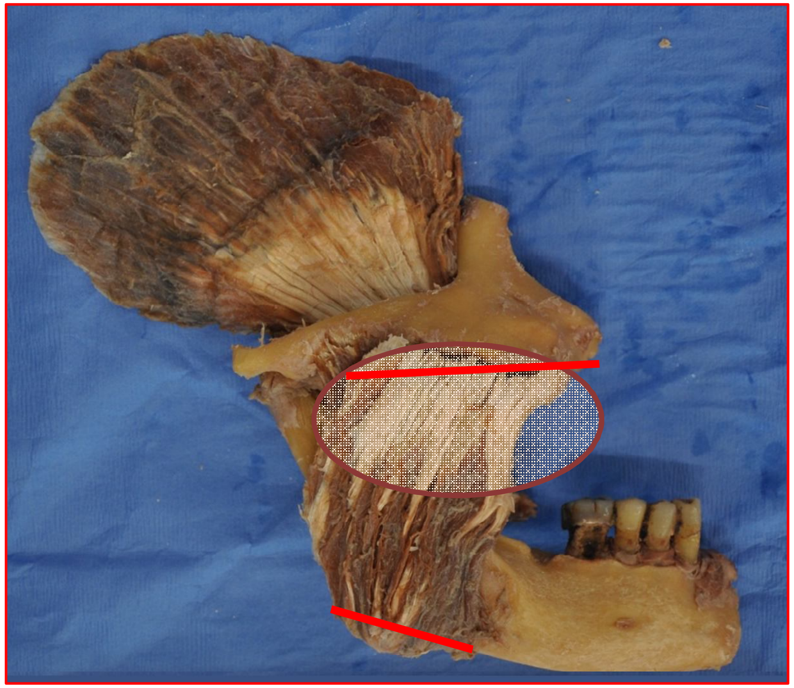

Modeling a "simple" muscle: the superficial masseter (3)

- Superficial layer:
  - Zygomatic insertion by a strong and thick aponeurosis → **quadrilateral with an edge along the zygomatic line**
  - Maxillar insertion

- Deep layer:
  - Maxillar insertion by an aponeurosis→ **quadrilateral with an edge on the along the maxillar line**
  - Zygomatic insertion

- Muscle belly composed of **straight fibers** linking **consistently** the 2 quadrilaterals

Modeling a “simple” muscle: the superficial masseter (4)

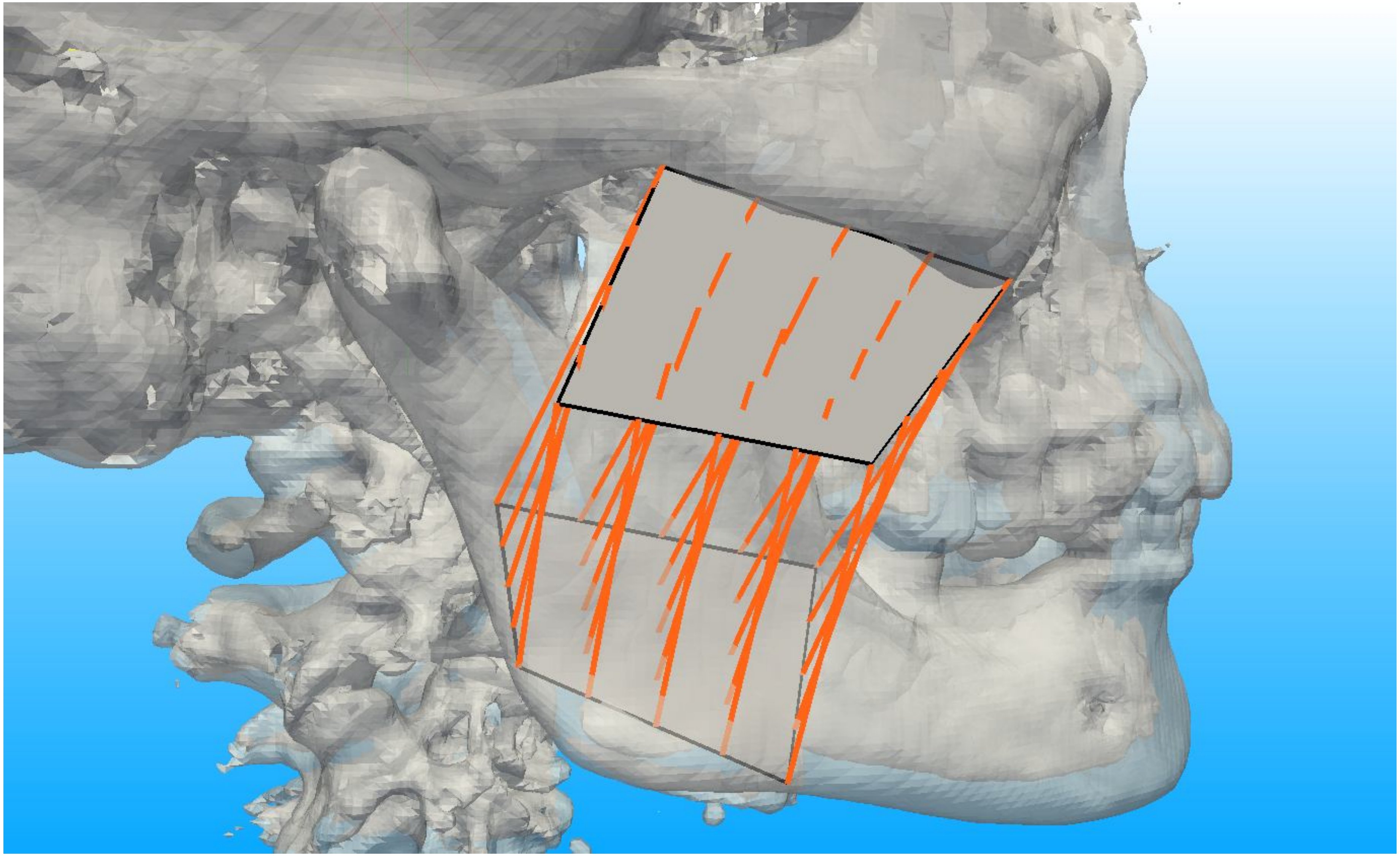

Woman, around 70 y. CT-Scan (497 x 512 x 512 / voxel size= 0.488281 x 0.488281 x 0,40 mm

Modeling a “simple” muscle: the superficial masseter (4)

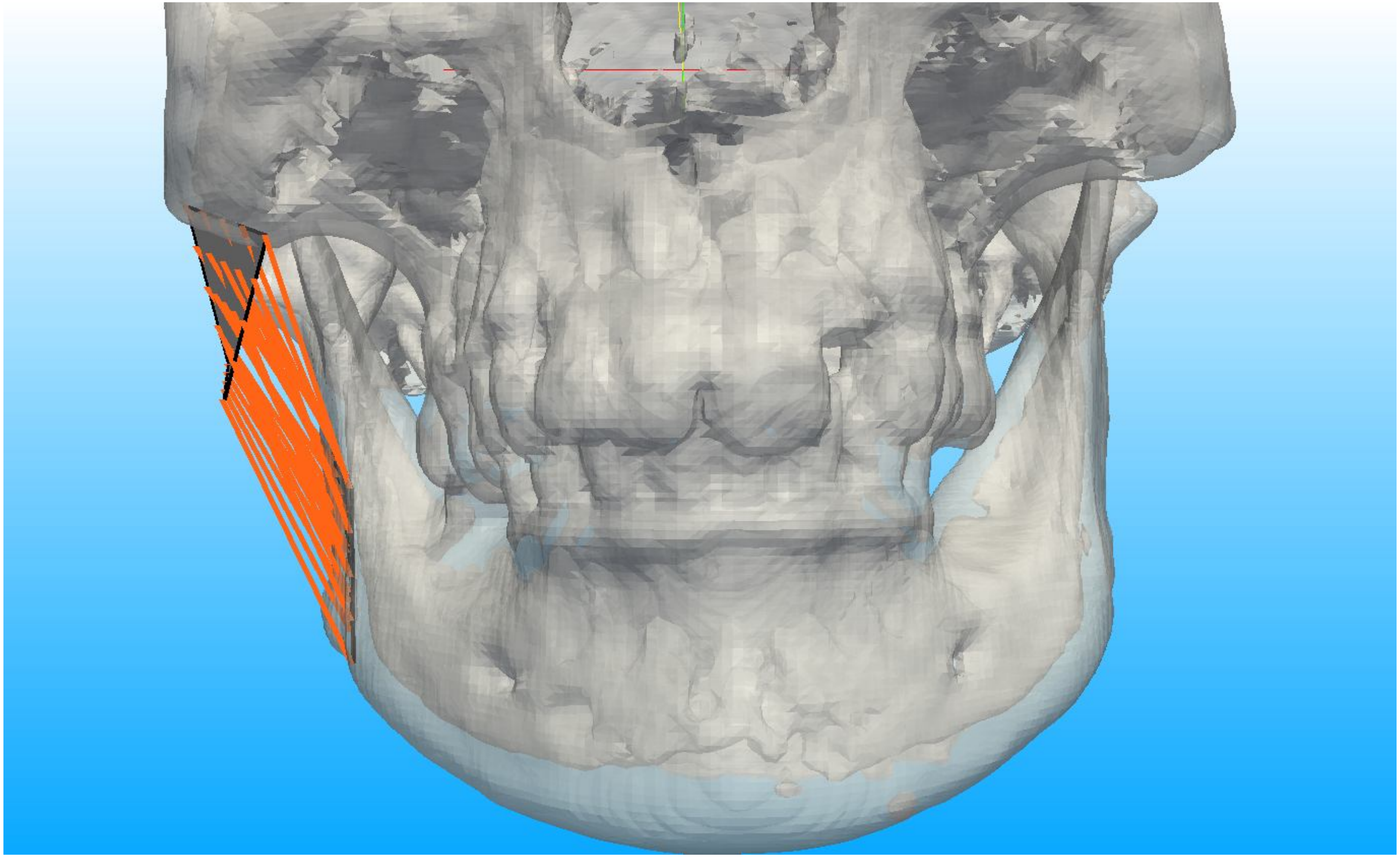

Modeling a "simple" muscle:
the superficial masseter (4)

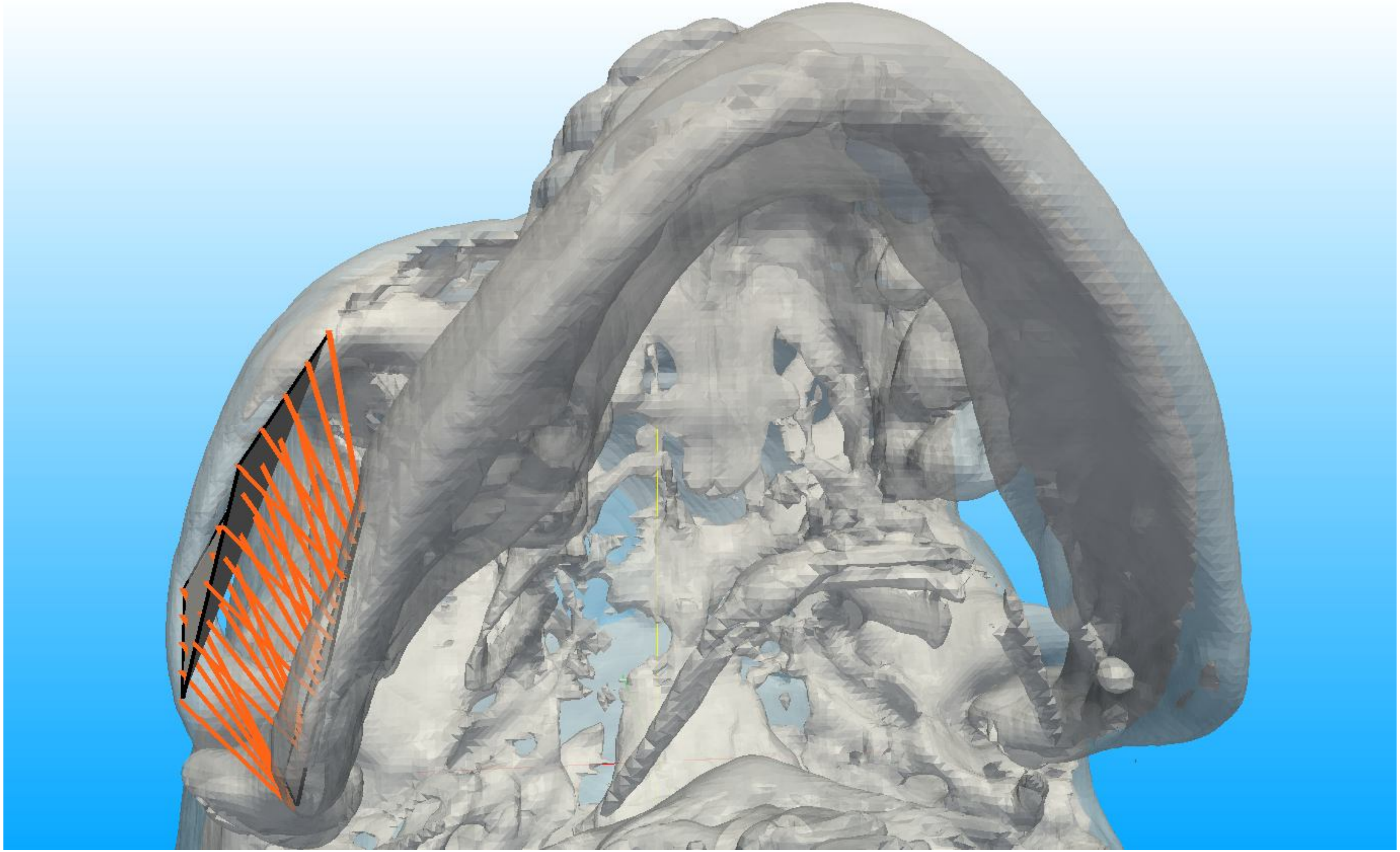

Modeling a “simple” muscle: the superficial masseter (4)

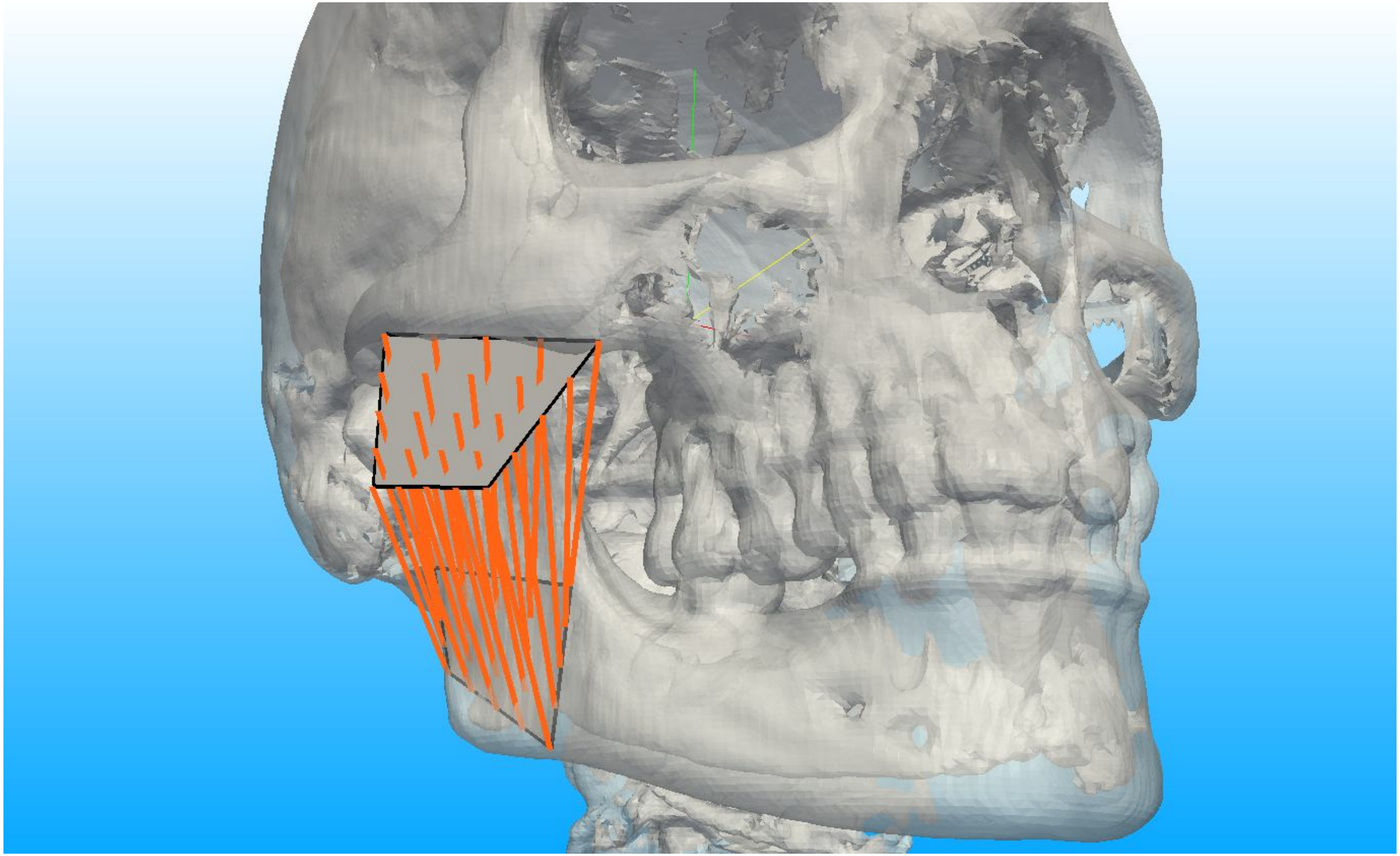

Modeling a “simple” muscle:
the superficial masseter (5)

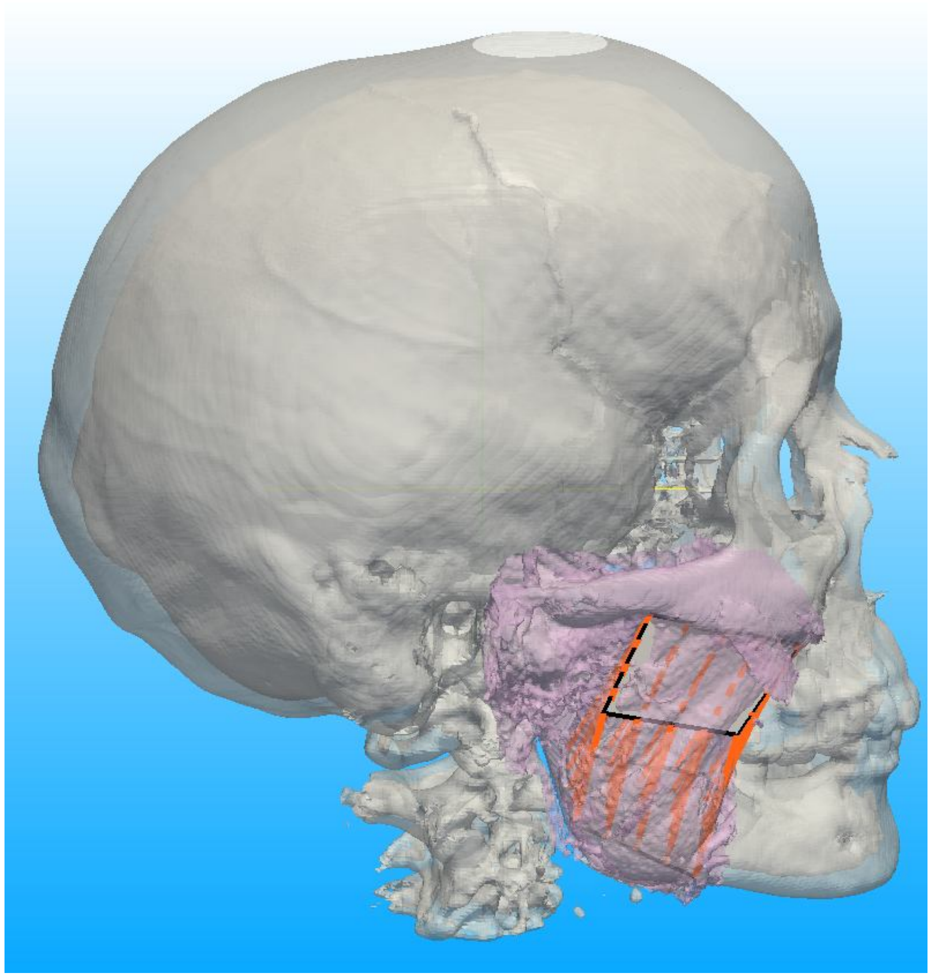

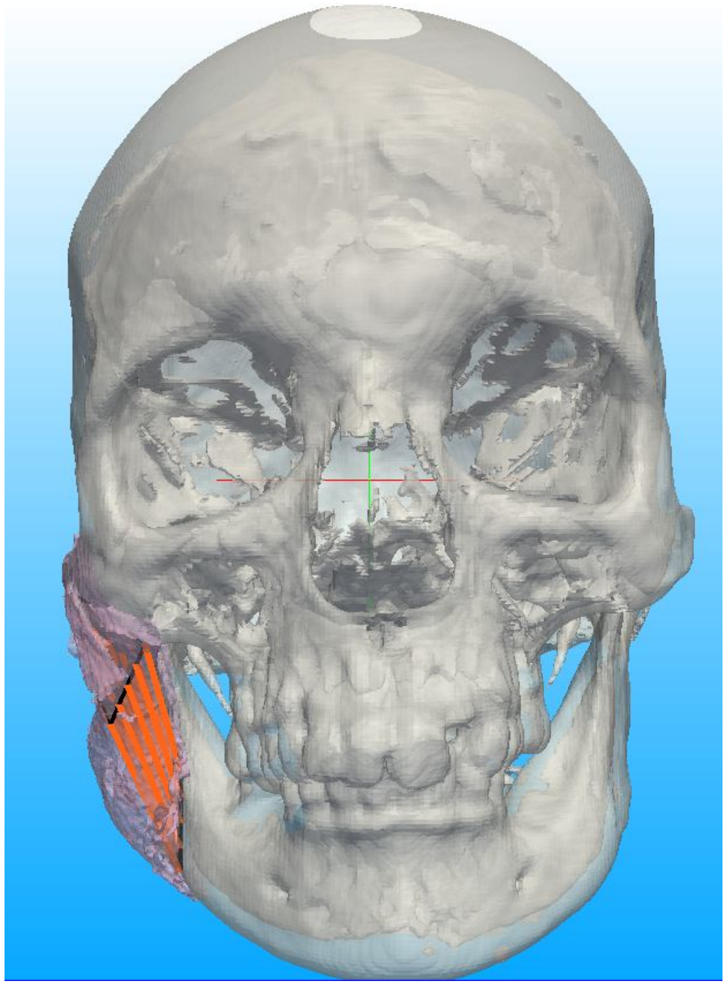

Rough segmentation of the soft tissue around masseter, by thresholding.

Modeling a “simple” muscle: the superficial masseter (6)

Computer Methods in Biomechanics and Biomedical Engineering, Vol. 9, No. 6, December 2006, 387–398
Taylor & Francis

Computational model of the movement of the human muscles of mastication during opening and closing of the jaw

LAETITIA M. M. LEON†, BERNARD LIEBGOTT‡*, ANNE M. AGUR‡ and KENNETH H. NORWICH†

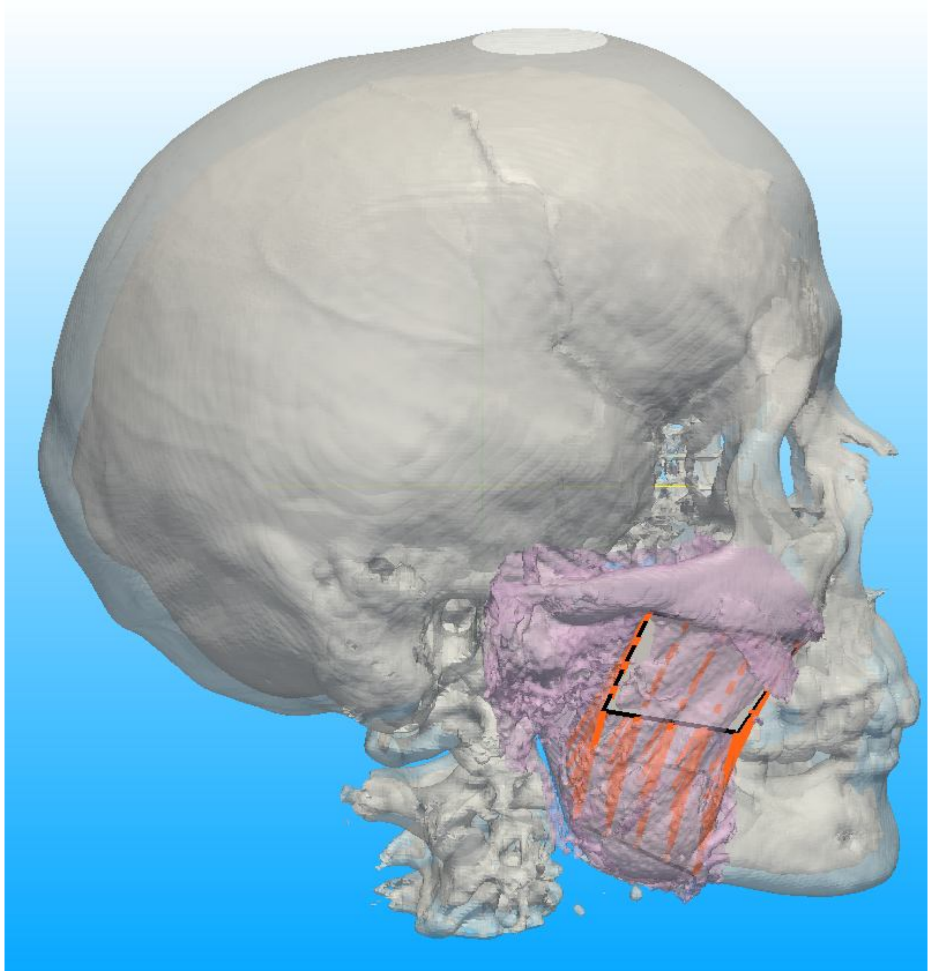

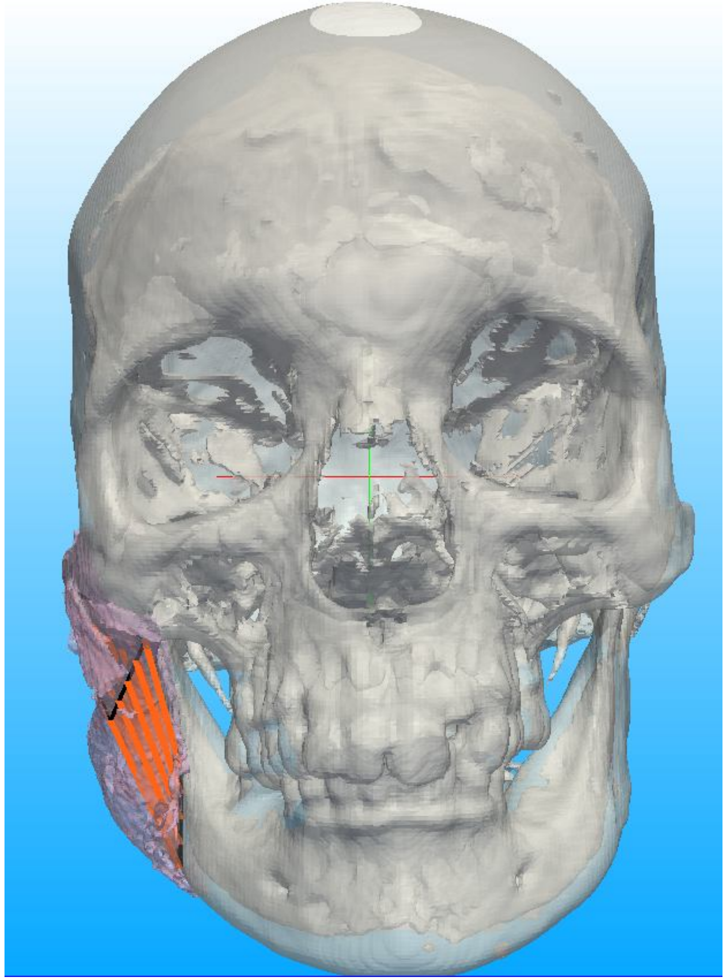

Fiber length in mm = 32.28 in [28.60, 35.21]
[Leon et al., 2006] = 30,16 (superficial) / 26,49 (deep)

Modeling a “simple” muscle: the superficial masseter (6)

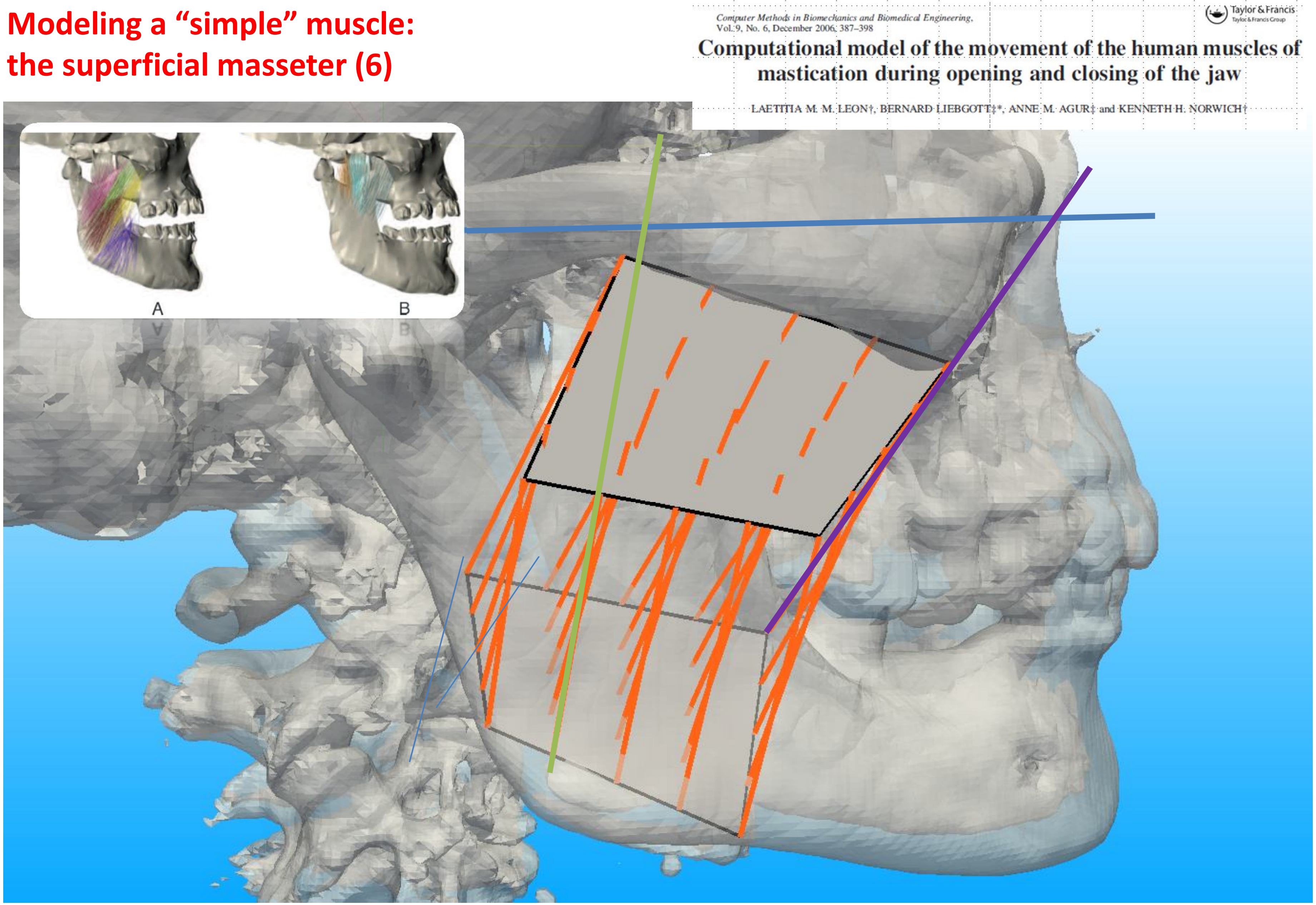

Fiber angle in degrees = 54 to 80
[Leon et al., 2006] = 51.61 (superficial) / 85.84 (deep)

Modeling a "simple" muscle:
the superficial masseter (7)

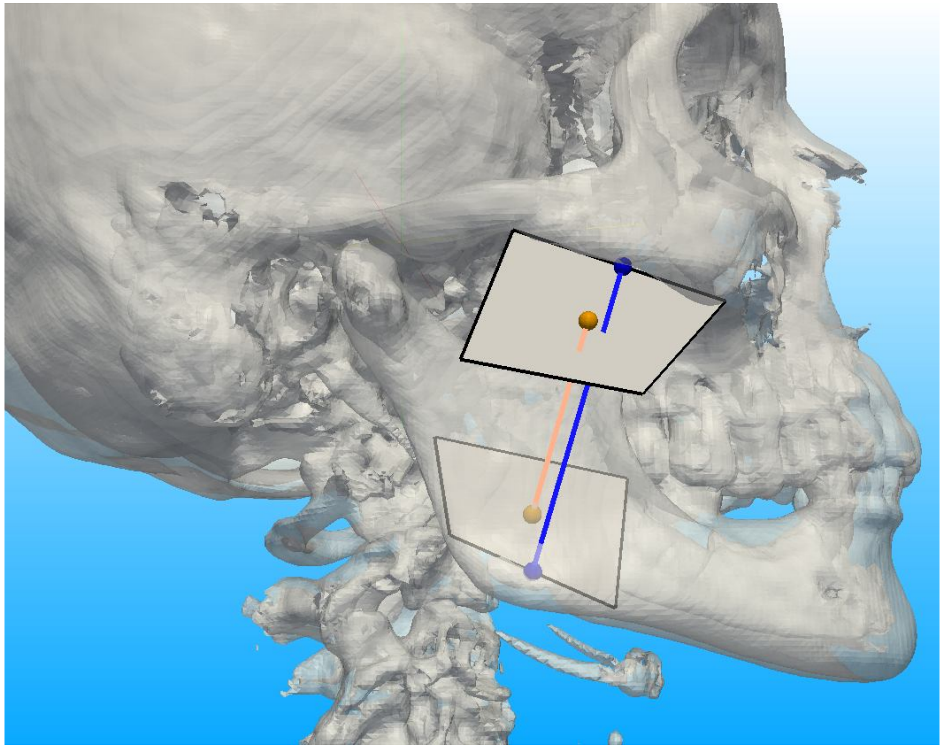

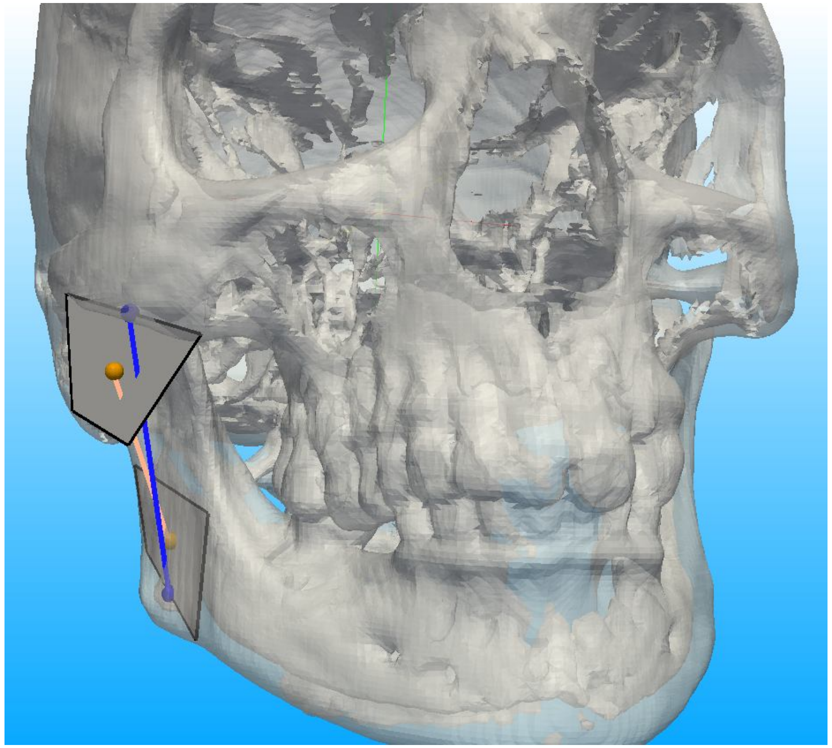

Comparison with a straight line of action representation:

- Fiber length in mm = 32.28 / LoA in mm = 49.99
- Completely different direction

→ Should be tested with the same biomechanical law (Hill-based) to analyze differences.

How to model aponeurosis (and… tendons) ?

COMPUTER METHODS AND PROGRAMS IN BIOMEDICINE 88 (2007) 112–122

ELSEVIER journal homepage: www.intl.elsevierhealth.com/journals/cmpb

Computational representation of the aponeuroses as NURBS surfaces in 3D musculoskeletal models

Florence T.H. Wu[a], *Victor Ng-Thow-Hing*[b], *Karan Singh*[c], *Anne M. Agur*[d], *Nancy H. McKee*[e,*]

ELSEVIER

Journal of Biomechanics 39 (2006) 2020–2025

JOURNAL OF BIOMECHANICS

www.elsevier.com/locate/jbiomech
www.JBiomech.com

Should tendon and aponeurosis be considered in series?

Marcelo Epstein[a], Max Wong[b], Walter Herzog[c,*]

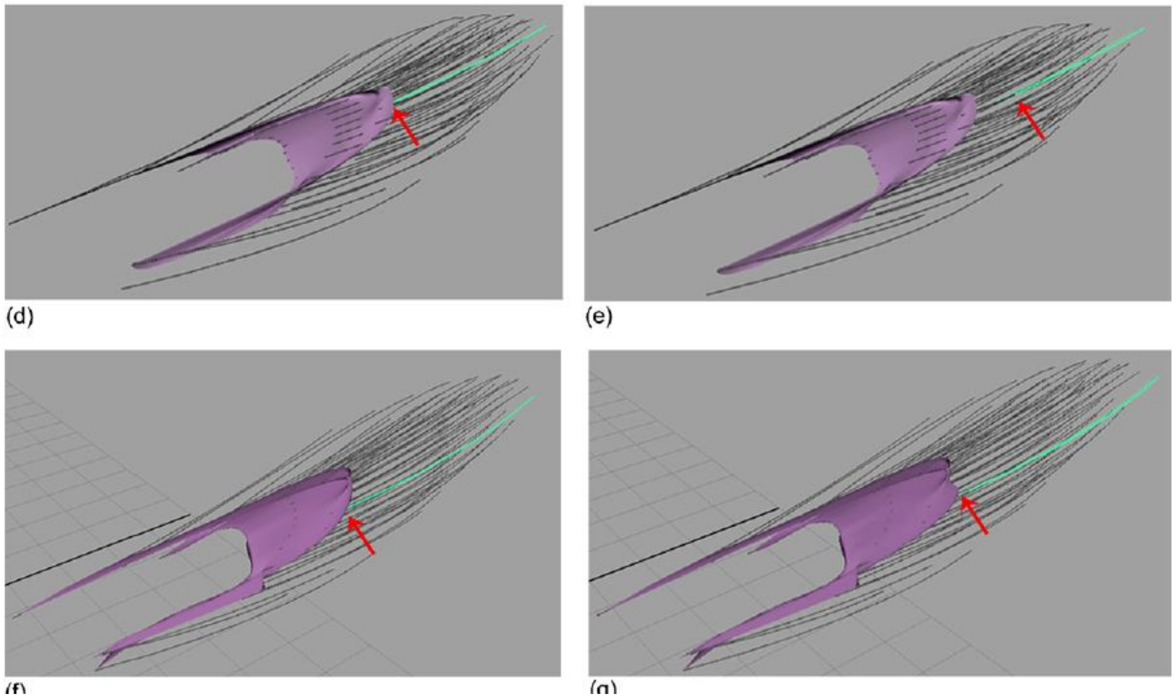

How to measure the physical parameters?

- Huge variability
- May vary w.r.t. to the age

Adjustment of Muscle Mechanics Model Parameters to Simulate Dynamic Contractions in Older Adults

Darryl G. Thelen

70 / Vol. 125, FEBRUARY 2003 Copyright © 2003 by ASME Transactions of the ASME

- How to define the optimal length (= rest length ?) in a configuration of several interacting muscles?